

FLOW-INDUCED FLUTTER OF SLENDER CANTILEVER HIGH-COMPLIANCE PLATES

Arvind Deivasigamani*, Jesse McCarthy*, Simon Watkins*, Sabu John*, Floreana Coman**

* School of Aerospace, Mechanical and Manufacturing Engineering, RMIT University
GPO Box 2476, Melbourne, Victoria, 3001, Australia

**FCST Pty. Ltd., P. O. Box 122, Melbourne, VIC 3053, Australia.
arvind.deivasigamani@student.rmit.edu.au

Keywords: *Flow-induced flutter, critical flutter velocity, flutter frequency*

Abstract

In this paper, the theory of flutter of slender cantilever plates in a fluid flow is discussed. Equations of motion of fluid-induced flutter are explained. The factors influencing critical flutter speed and flutter frequency of these beams are determined theoretically. Scaling laws are established for flutter frequency and onset velocity based on the material and fluid properties.

Experiments are conducted to validate the scaling laws with paper, polypropylene and Mylar of different lengths. The experimental results follow the same trend as the scaling laws. Based on the obtained results, constant of proportionalities are inserted to the scaling laws. The effect of leading edge clamping conditions on the critical flutter velocity is also discussed.

1. Introduction

Flutter of flags, sails and other slender plates and beams have always been a very interesting problem in the field of fluid structure interaction over the years. It is not only a day-to-day phenomenon, but also has complex science involved in its behaviour that interests many scientists and engineers [1]. Some of the earliest work in this regard was carried out by Lord Rayleigh [2] to theoretically prove the instability of an elastic plate of infinite dimensions immersed in axial potential flow.

However, these theories were not exactly applicable to explain the flutter of plates of finite dimensions. After the inventions of high-speed flights, it was essential to look into this fluid structure problem again. In this regard, Theodorsen [3] provided mathematical explanations to the theory of flutter and aerodynamic instability. Since then, there has been plenty of work in determining the flutter behaviour analytically, numerically and also experimentally [4-7].

Flutter of slender, cantilevered, high-compliance plates of finite length are well understood in recent years. It is evident that there exist distinct states of flapping observed in these plates [8]. Initially, the plate has a fixed-point stability and as the flow velocity increases, a transition to limit cycle flapping and then, chaotic flapping is observed. Thus, it is essential to determine the critical flutter velocity in terms of solid and fluid properties.

Huang [9] investigated the flutter of cantilever plates in axial flow for possible treatment of patients having snoring problems due to flutter of palates. In this work, a linear beam model with Theodorsen's principle was used to determine the critical flutter velocity and flutter frequency of the plates. Yamaguchi et al. [10,11] and Watanabe et al. [12,13] conducted a large number of experiments to determine the factors influencing the critical flutter velocity.

Argentina and Mahadevan [14] investigated the flutter behaviour of cantilevered plates in axial flow using linear beam model and a simplified model based on Theodorsen's

theory of flutter. The pressure difference determined in this analysis is valid for an inviscid, incompressible flow for small-amplitude motions. It also accounts for finite length of the plate, vortex shedding and fluid-added mass. More interestingly, they provide simple scaling laws for critical flutter velocity and flutter frequency and highlight the relationship between the critical flutter onset velocity and the plate's natural frequency. It is also evident that these scaling laws match with the findings from other researchers (discussed in the next section).

While these works remain as a study of this natural phenomenon, fluid induced flapping has found its application in energy harvesting in recent years. Allen and Smits [15] proposed an energy harvesting system that suggests the possibility of having a piezoelectric 'eel' in the wake of an upstream bluff body, which can shed vortices that impinge on the eel and thereby inducing flutter in the piezoelectric membrane. Since piezoelectric membranes have the ability to generate electrical charge upon mechanical strain, exploitation of fluid induced fluttering is conceivable. Pobering and Schwesinger [16] examined a micro-structured, piezo-bimorph placed in unstable flow for energy harvesting. Due to the constant upward and downward bending of the piezo, electric power was generated and stored. It was mentioned that these devices could be scaled according to the power requirement.

Dickson [17] suggested a concept of piezoelectric tree where flexible piezo elements could be coupled with leaf-like polymers and arranged to give a tree-like appearance. Li and Lipson [18] investigated this leaf stalk system experimentally by using a PVDF stalk and a triangular leaf connected by a free hinge. It was mentioned that this connected body was efficient at low wind speeds and the leaf amplifies the flutter behaviour of the piezo-stalk.

Some of the other recent work on energy harvesting from fluid induced flapping include the work done by Hobeck and Inman [19] and Bryant et al. [20]. Hobeck and Inman attempted to develop a piezoelectric grass concept where the grass could flap and generate electrical

power at low velocity, highly turbulent water flow. Bryant et al. used a connected body system with a hinge and piezo film attached to the clamped end of the cantilever beam. Two such devices were placed parallel to the wind flow and the wake interactions between the devices are explained.

In this paper, a brief explanation for flutter of simple cantilever plate of finite length based on Theodorsen's theory [3] and Argentina and Mahadevan [14] is given. The system parameters, which affect the critical flutter onset velocity and flutter frequency, are explained. The scaling laws and relationships from the literature are mentioned and ways to alter critical flow velocity and flutter frequency of the structure for energy harvesting applications are theoretically discussed.

Experiments are carried out in order to determine the material and fluid properties responsible for critical flutter velocity and its flapping frequency. Three different materials (paper, polypropylene and Mylar) are tested with various different cantilever lengths in order to vary the cantilever length, mass density and stiffness mentioned in the scaling laws. Critical flutter velocity and frequency are experimentally determined and compared with their corresponding scaling laws.

Constant of proportionalities are introduced in the scaling laws based on the obtained results. The three-dimensional effects in experiments are also discussed in brief. The effect of clamping width and clamping length conditions on critical flutter velocity are experimentally determined and the results are provided.

2. Theory of flutter

The governing equations of flutter of a simple cantilever plate of finite length are given by Argentina and Mahadevan [14]. The flow considered in this two-dimensional analysis is inviscid and incompressible. Although it does not include the nonlinearities in the system, it accounts for the finite length of the plate, vortex shedding at the trailing edge and the fluid-added

mass. The basic theory and equations of this work are given below.

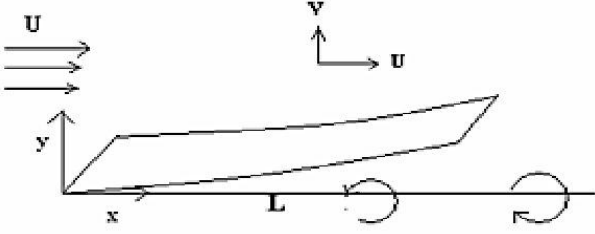


Fig. 1. Schematic representation of a flapping plate indicating vortex shedding at trailing edge.

The causation of flutter here is the pressure difference across the upper and lower surfaces of the plate. The Euler-Bernoulli beam equation of motion is given by

$$m \frac{\partial^2 y}{\partial t^2} + EI \frac{\partial^4 y}{\partial x^4} = w \Delta P \quad (1)$$

Where $m = \rho_s h l$; m - mass per unit length of the plate, ρ_s - density of the plate, h - thickness of the plate, w - width of the plate, E - Young's modulus, I - moment of inertia, ΔP - pressure difference across the plate due to the fluid flow. The pressure difference, according to Theodorsen [3], is divided into circulatory pressure (P_c) and non-circulatory pressure (P_{nc}).

$$\Delta P = P_{nc} + P_\gamma \quad (2)$$

The small deflections of the plate create a transverse velocity and thus a velocity potential. Thus, based on the airfoil theory [21], the non-circulatory pressure according to linearised Bernoulli equation is given by

$$P_{nc} = -2\rho_f \frac{\partial^2 y}{\partial t^2} \sqrt{x(L-x)} + \frac{\rho_f U(2x-L)}{\sqrt{x(L-x)}} \left(\frac{\partial y}{\partial t} + U \frac{\partial y}{\partial x} \right) \quad (3)$$

where ρ_f - density of the fluid. The circulatory pressure is created due to the vortex shedding at the trailing edge of the plate. According to Kelvin's theorem, vorticity has to be conserved in an inviscid flow for a given topology. Therefore, to conserve the total vorticity, if there is a vorticity distribution at the wake of the plate, it should be balanced by a bound vorticity

distribution in the plate with opposite strength (as shown in figure 1). This creates a circulatory velocity potential whose finite variation at the trailing edge is governed by the Kutta-Zhukovskii condition [22]. Thus, the circulatory pressure is given by

$$P_c = \frac{-\rho_f U}{\sqrt{x(L-x)}} \left(\frac{\partial y}{\partial t} + U \frac{\partial y}{\partial x} \right) [L(2C-1) + 2x(1-C)] \quad (4)$$

where C is the Theodorsen functional given by

$$C = \frac{\int_1^\infty \frac{x_o \gamma dx_o}{\sqrt{x_o^2 - 1}}}{\int_1^\infty \frac{\sqrt{x_o + 1}}{\sqrt{x_o - 1}} \gamma dx_o} \quad (5)$$

Here, γ is the vortex strength and x_o is the non-dimensional number based on the position of vortices.

When a cantilever plate is placed in a fluid flow and the flow velocity is increased, the plate initially remains stable and then begins to flutter at a particular fluid velocity. This velocity is called as the critical flutter velocity (U_c). Argentina and Mahadevan provided a simple explanation to determine the system parameters responsible for flutter frequency and critical flutter velocity. According to their explanation, when a rigid plate (hinged at the leading edge) oscillates, the fluid pressure through a small angle should equal to the inertia of the oscillating plate. Fluid pressure through a small angle, θ , is given by $\rho_f U^2 \theta$. When this equals the inertia of the oscillating plate given by $\rho_s h \omega^2 L \theta$, the flutter frequency is scaled as

$$\omega \sim \sqrt{\frac{\rho_f U^2}{\rho_s h L}} \quad (6)$$

When the fluid pressure is large enough to excite a resonant bending mode, the plate begins to flutter. Therefore, when we equate the flutter frequency to the natural frequency, the scaling law for critical flutter velocity is given as

$$U_c \sim \sqrt{\frac{E h^3}{\rho_f L^3}} \quad (7)$$

Although these are scaling laws, the system parameters affecting the critical flutter velocity are clearly stated. Also, the relationship between the critical flutter velocity and the natural frequency of the plate is established. Since the pressure across the plate should be able to excite the lowest resonant bending mode, the critical flutter velocity is directly proportional to the plate's natural frequency. Huang [9] also states the critical flutter velocity as a function of beam's stiffness, density and its cantilever length, which matches with the above scaling law.

Structural engineers prefer to design the structure with higher flexural rigidity and lower cantilever length in order to avoid flutter. However, for applications of piezoelectric energy harvesting from fluid flow, it is essential for the piezoelectric patches to flutter at low flow velocities commonly observed in the environment. Also, for energy harvesting in urban areas, the critical flutter velocity should be around 2-5m/s as these are the average wind speeds observed in urban areas [23].

Since the density of air is relatively low to reduce the critical flutter velocity, the structural parameters have to be altered to reduce flutter velocity. Unfortunately, these piezoelectric materials have a certain stiffness and density which cannot be modified to suit this application. Thus, the cantilever length of these piezoelectric beams has to be increased in order to excite its resonant bending mode. However, increasing the piezoelectric beam's length would not prove to be cost effective. Also, the frequency of flutter would reduce and thus reduce the power output.

In order to overcome the above limitations, attaching a compliant material to the trailing edge of the piezo beam could increase the overall cantilever length. Li and Lipson (2009) have attached a polymeric material (called the 'leaf') to the trailing edge of the PVDF piezo beam with the help of a free hinge. It is mentioned that this arrangement increases the power output as the leaf amplifies the fluid induced flutter. Bryant et al. (2011) have experimented their energy harvesting device with a similar arrangement.

Thus, for various applications, it is vital to understand the theory of flutter and to determine the factors causing them. This would also help in altering the system parameters to achieve flutter at low wind speeds or to avoid it based on the application. In the next section, experimental validation of these scaling laws is provided.

3.Experimental validation

In order to assess the extent to which the theoretical scaling laws are valid, experiments are performed in industrial wind tunnel. Since, the factors involved in the scaling laws include material stiffness, density and geometry, different materials with various cantilever lengths were tested. The experimental setup and procedure are explained in this section.

3.1 Experimental setup

The wind tunnel used for the experiments has an octagonal test cross-section of 1.32 x 1.07m. The test section is 2.1m long and is powered by a 134-horsepower DC motor driving a six bladed fan. The maximum speed of the wind tunnel is found to be 45m/s with a contraction ratio of 4:1 and turbulence intensity less than 1%. Thus, all the experiments are carried out in smooth flow.

The test samples used for experiments include polypropylene, paper and Mylar. Tensile tests were performed to obtain the modulus for these materials. Properties of these materials are listed in table 1. All the test samples used for the experiments have a common width of 60mm and thickness of 0.35mm. The cantilever lengths of these materials are varied from 118mm (considered as L) to 283.2mm (2.4L). Thus, the lengths are varied from L to 2.4L in steps of 0.1L, thereby providing 15 samples of each material.

The test samples are clamped at the leading edge with the help of two metal strips held vertically by a stand such that the samples flutter in parallel flow. It is ensured that the stand is placed far away so as to not disturb the flow and motion of the flapping plates. The

dimensions of the metal clamping strips are varied to observe its effect on the critical flutter velocity. The clamping strips are guyed with very thin metal wires to the tunnel walls to avoid any vibrations of the upstream clamping system due to the flow or flutter of the samples.

A high-speed camera (IDT X-Stream XS4) is placed far downstream facing the samples in order to shoot the flutter at 1000 frames per second, which is high enough to capture the flutter frequency of all the samples. The camera captures and stores the images locally, obviating any buffering time delay. The velocity in the tunnel is measured with a pitot-static tube. A picture of the set up is shown in figure 2.

Table 1. Material properties of the test samples

Material	Young's Modulus (Mpa)	Density (kg/m ³)
Polypropylene	1261	995
Paper	2124	773
Mylar	3000	1400

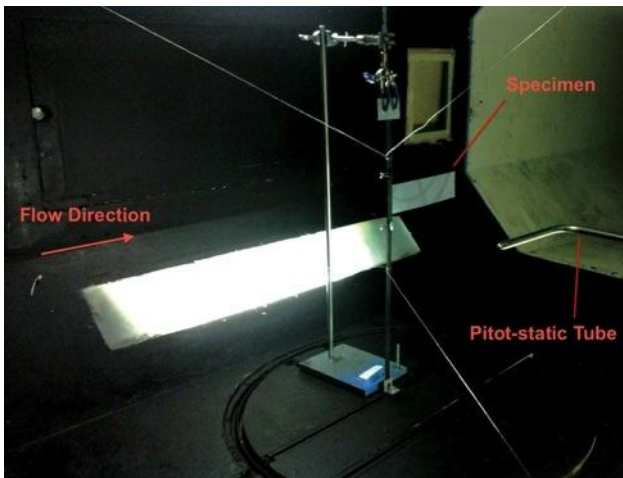


Fig. 2. A typical experimental setup in the wind tunnel.

3.2 Experimental procedure

After the test rig and camera were setup in the wind tunnel, another pitot-static tube was placed at the position of the actual sample to compare the pressure values. A blockage correction factor of 1.1 was observed and this factor was incorporated in all the results. The clamped length of all the samples is 0.1L at the leading edge.

Each of the samples was clamped (as shown in figure 1) and the wind speed was gradually increased. Since the transition of the structure from fixed-point stability to steady state flapping occurs at a unique flow velocity, it was clearly determined by visual inspection and this flow velocity (U_c) was noted. This procedure was repeated three times to ensure accuracy in the results.

Once the critical flutter velocity is reached for the shortest sample (L_b) and the sample flutters at a steady state, the high-speed camera is turned on and the flutter of the sample is captured for 5 seconds (i.e. 5000 frames). The video footage was then transferred to the computer. This procedure is repeated for all the samples. Flutter frequency of each material, having different cantilever lengths, were measured at a constant flow velocity. Therefore, the samples tested for flutter frequency were limited in each material (discussed in next section). The videos were processed later using *Motion Studio* to determine the flapping frequency. A picture taken from the high-speed footage is shown in figure 3.

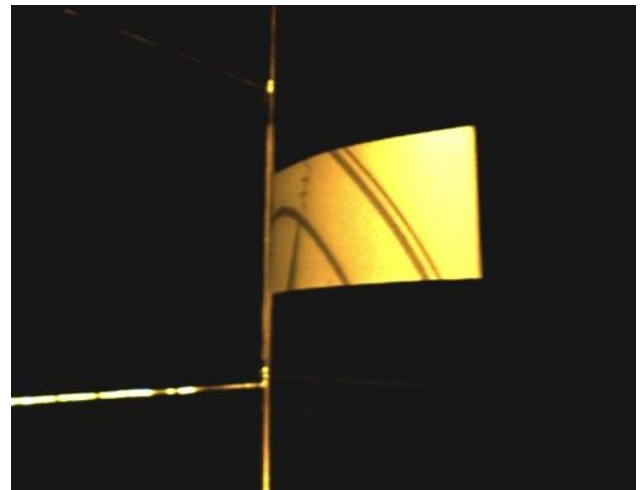


Fig. 3. A screen shot of polypropylene (1.7L) in motion.

4. Results and Discussion

Based on the experiments carried out with various different samples, the critical flutter velocity and flutter frequency are determined and its relationship with different system parameters and theoretical laws are discussed in the following sections.

4.1 Critical flutter Velocity

It is well known from theory that critical flutter velocity (U_c) is a unique velocity at which the structure transitions from the static stable condition to steady state flapping. In the experiments performed, the cantilever length of the samples was varied from L to $2.4L$ and the critical flutter velocity is distinctively observed for each sample. These observed values are plotted against the non-dimensional lengths of the samples. Figure 4 shows the results of the critical flutter velocity of polypropylene and paper of non-dimensional lengths, 1 to 2.4.

Since the Mylar samples have very high modulus and density, shorter samples of this material was observed to have a very high U_c that went beyond the safe limits of the wind tunnel. Also, due to the high flexural rigidity and plastic nature of the material, longer samples had a snapping tendency while fluttering. Thus, Mylar sample results are not included here.

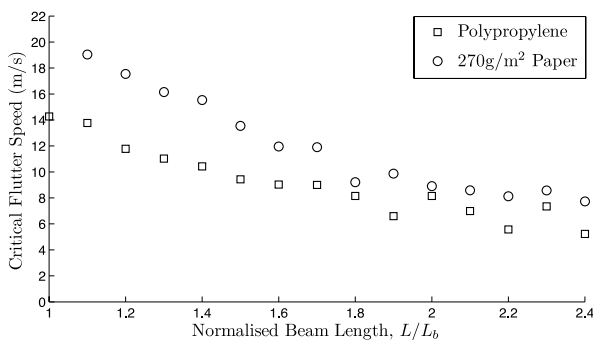


Fig. 4. Experimental critical flutter speed of polypropylene and paper of different lengths.

From figure 4, it is evident that as the cantilever length increases, U_c decreases for both paper and polypropylene. When the length of the samples is shorter, U_c is distinctively higher and clearly determined as the transition from static stability to flutter occurs instantaneously. However, as the cantilever length is increased, the transition from static stability to steady flapping takes few seconds making it difficult to define U_c . Also, the flow velocity is very low indicating that the samples of longer lengths are highly unstable. This could be attributed for the values not following a

specific trend when lengths of samples are longer. Also, it is clearly visible that paper, being rigid, flutters at higher U_c .

In figure 5, the experimental results are compared with the theoretical scaling laws for U_c of polypropylene and paper. From equation (7), it is known that

$$U_c = K_1 \sqrt{\frac{Eh^3}{\rho_f L^3}} \tag{8}$$

where K_1 is a constant of proportionality. The scaling law U_c values are plotted with $K_1 = 1$. It is clearly evident that the experimental results clearly follow the same trend of the scaling laws. This implies that there exists a constant of proportionality, K_1 irrespective of the structure material and geometry.

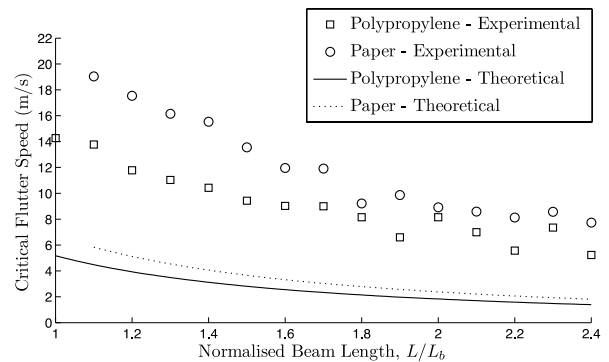


Fig. 5. Comparison of experimental results of critical flutter speed with corresponding scaling laws.

Based on the experimental results, the constant of proportionalities are worked out for every sample by calculating the ratio of experimental U_c to theoretical U_c . It is observed that the average K_1 value for polypropylene is 3.618 and that of paper is 3.784. Ideally, the values should have been exactly the same. However, since the critical flutter speed could not be clearly defined for long lengths, it could have resulted in a small difference in K_1 values. The K_1 values of both the samples of different lengths are shown in figure 6. It is seen clearly that the values are relatively stable as expected. Thus, this constant value could be used to predict the critical flutter speed for any material of wide range of cantilever lengths.

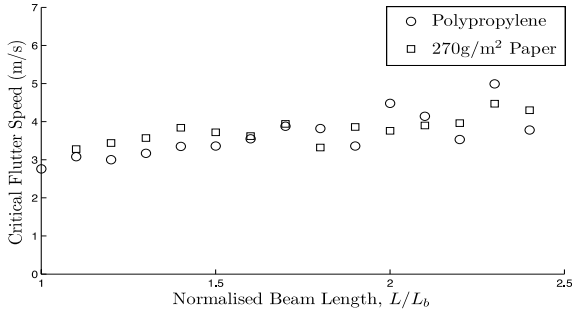


Fig. 6. K values of critical flutter speed for different samples versus its normalized lengths.

4.2 Flutter frequency

Flutter frequency of a structure induced by fluid flow could be measured only after the structure transitions from static stability to steady state flapping. Also, in order to determine the flutter frequency as a function of material properties and geometry, it is important to record the flutter frequencies at a constant wind speed for each material. It is also known that as the flow velocity increases, the pressure difference across the plates is extremely high. Thus, the structure transitions to chaotic flapping. Therefore, longer lengths of these samples transitioned to chaotic flapping and hence had to be neglected for this analysis.

Figure 7 shows the flutter frequency of paper and polypropylene of different normalized lengths. From the figure, it is clear that as the cantilever lengths increase, the flutter frequency reduces as expected from the scaling laws. Also, since paper has a high modulus, the flutter frequencies are higher compared to that of polypropylene. The cantilever lengths are chosen such that the frequencies could be recorded at constant wind speed.

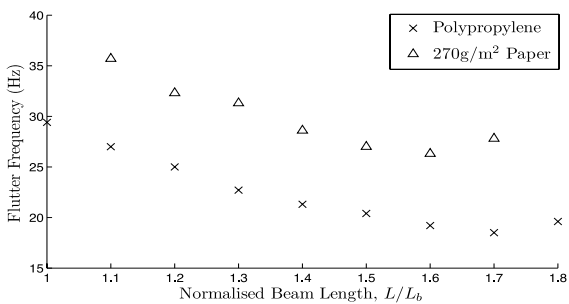


Fig. 7. Experimental flutter frequency of polypropylene and paper of different lengths.

In figure 8, these experimental flutter frequency values are compared with theoretical scaling laws. From equation (6), we know that

$$\omega = K_2 \sqrt{\frac{\rho_f U^2}{\rho_s h L}} \quad (9)$$

where K_2 is a constant of proportionality. The scaling laws are plotted for $K_2 = 1$. It is evident that the experimental results follow the same trend of scaling laws. This indicates that a constant of proportionality could be worked out for flutter frequency irrespective of the material properties and geometry.

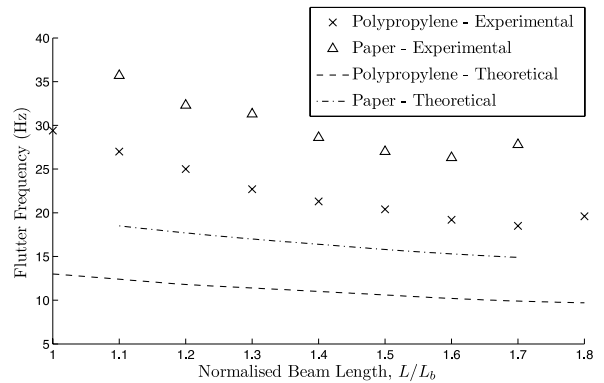


Fig. 8. Comparison of experimental results of flutter frequencies with corresponding scaling laws.

The K_2 values are determined in a similar manner as that of K_1 and it is observed that the average K_2 values are constant irrespective of the material stiffness and geometry. It is observed that the average K_2 value for polypropylene is 2.02 and that of paper is 1.81. Ideally, the values should have been exactly the same. This difference in the values could be attributed to the inaccuracies in high-speed footage. Also, the longer lengths could flutter in a combination of modes making it difficult to determine the frequencies accurately. The K_2 values of both the samples of different lengths are shown in figure 9. It is seen clearly that the values are relatively stable as expected. This indicates that for a given width of the plate of any material, flutter frequency can be predicted for a wide range of cantilever lengths.

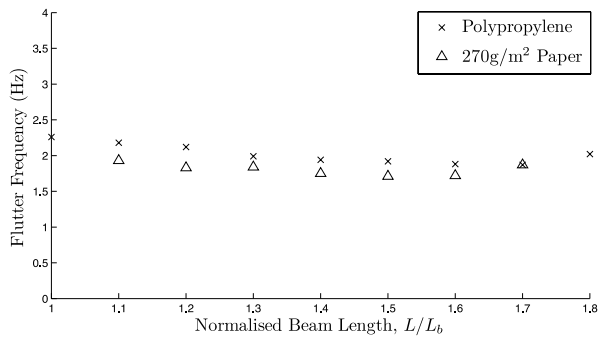


Fig. 9. K values of flutter frequency for different samples versus its normalized lengths.

Based on the K values calculated, some of the Mylar samples' flutter frequencies were theoretically predicted and compared with the experimental results. The findings are listed in table 2. The predictions match closely with the obtained results.

Table 2. Comparison of experimental and theoretical results for 3 samples of Mylar

Normalized lengths	Observed flutter frequency (Hz)	Predicted flutter frequency (Hz)
1.6	21.3	21.2
1.7	20	20.4
1.8	18.8	20

One aspect that has not been studied is the width of these test samples. In all the tests, the width of the sample is maintained constant. This is because, the theoretical scaling laws are obtained based on a two dimensional analysis. However, it is expected that as the width increases, the plate would become increasingly unstable.

4.3 Effect of clamping conditions

One important aspect that has not been considered in theoretical modeling and also by other researchers is the effect of the leading edge clamping conditions. These clamps could shed vortices downstream and affect the flutter behaviour of the test samples.

In this work, the effect of leading edge clamping width and length on critical flutter velocity is considered. Clamping lengths were varied from 20 to 75mm and it was observed

that its effect on critical flutter velocity was negligible. However, when the clamping width was varied, a considerable change in the critical flutter velocity was observed. Figure 10 shows that as the clamping width is increased, U_c increases. It is believed that due to the vortex shedding of the clamps on both sides of the plates downstream, the flutter is delayed, making the sample more stable. The work done here is a preliminary study to observe the effect of the clamping conditions. A more detailed study is however required to understand the effect of vortex shedding on the flutter behaviour.

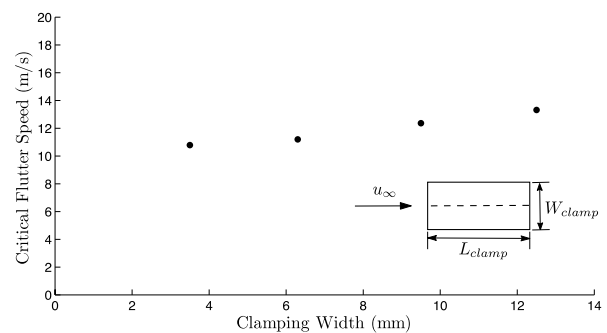


Fig. 10. Effect of clamping width on critical flutter speed

5. Conclusion

The flutter behaviour of slender, high compliance cantilever plates are understood from the literature and the scaling laws for critical flutter velocity and flutter frequency are established based on the material and fluid properties.

Experimental results show that the critical flutter speed and flutter frequency align well with the scaling laws. Constant of proportionalities are established for these scaling laws to predict the flutter speed and frequency of a material with a known width. This confirms the dependence of critical flutter speed and frequency on the various system parameters, namely stiffness, density and geometry.

The results show that the critical flutter velocity could be increased or decreased by varying the material properties or geometry based on the application. This is a critical finding given the need to induce flutter for

nominal wind speeds of 2-5 m/s in most urban areas. The limitations of the two dimensional scaling laws are indicated and the effect of leading edge clamping conditions on the flutter behaviour is also discussed. It is believed that this validation of the scaling laws could be useful for structural engineers to avoid fluid induced instability and to reduce critical flutter speed for energy harvesting applications by varying the required system parameters.

Acknowledgment

The authors would like to thank the Australian Research Council (ARC) for offering their support for this research through grant LP100200034.

References

- [1] Païdoussis M. *Fluid-Structure Interactions - Slender Structures and Axial Flow*. Vol. No. 1, Elsevier Academic Press, 1998.
- [2] Lord Rayleigh. On the instability of jets, *Proc. of London Mathematical Society*. Vol. No. 9, pp 4-13, 1879.
- [3] Theodorsen T. General theory of aerodynamic instability and the mechanism of flutter. *National Advisory Committee for Aeronautics*, Technical Report No. 496, 1949.
- [4] Datta S.K. and Gottenberg W.G. Instability of an elastic strip hanging in an airstream. *Journal of Applied Mechanics*, Vol. No. 42, pp 195-198, 1975.
- [5] Kornecki A, Dowell E.H. and O'Brien J. On the aeroelastic instability of two-dimensional panes in uniform incompressible flow. *Journal of Sound and Vibration*. Vol. No. 47 (2), pp 163-178, 1976.
- [6] Païdoussis M. *Fluid-Structure Interactions - Slender Structures and Axial Flow*. Vol. No. 2, Elsevier Academic Press, 2004.
- [7] Eloy C, Souilliez C. and Schouveiler L. Flutter of a rectangular cantilevered plate. *Proceedings of the Sixth FSI, AE & FIV + N Symposium, ASME PVP 2006/ICPVT-11 Conference*. Vancouver, Canada, 2006.
- [8] Connell B. S. H. and Yue D. K. P. Flapping dynamics of a flag in a uniform stream. *Journal of Fluid Mechanics*, Vol. No. 581, pp 33-67, 2007.
- [9] Huang L. Flutter of cantilevered plates in axial flow. *Journal of Fluids and Structures*, Vol. No. 9, pp 127-147, 1995.
- [10] Yamaguchi N, Sekiguchi T, Yokota K, and Tsujimoto Y. Flutter limits and behavior of a flexible thin sheet in high-speed flow—I: analytical method for prediction of the sheet behaviour. *ASME Journal of Fluids Engineering*. Vol. No. 122, pp 65-73, 2000.
- [11] Yamaguchi N, Sekiguchi T, Yokota K, and Tsujimoto Y. Flutter limits and behavior of a flexible thin sheet in high-speed flow—II: experimental results and predicted behaviors for low mass ratios. *ASME Journal of Fluids Engineering*. Vol. No. 122, pp 74-83, 2000.
- [12] Watanabe Y, Isogai K, Suzuki S, and Sugihara M. A theoretical study of paper flutter. *Journal of Fluids and Structures*. Vol. No. 16 (4), pp 543-560, 2002.
- [13] Watanabe Y, Suzuki S, Sugihara M, and Sueoka Y. An experimental study of paper flutter. *Journal of Fluids and Structures*. Vol No. 16 (4), pp 529-542, 2002.
- [14] Argentina M and Mahadevan L. Fluid-flow-induced flutter of a flag. *Proceedings of the National Academy of Sciences of the United States of America*, Vol. 102(6), pp1829-34, 2005.
- [15] Allen J.J. and Smits A.J. Energy harvesting eel. *Journal of Fluids and Structures*. Vol. No. 15(3-4), pp 629-640, 2001.
- [16] Pobering S and Schwesinger N. A novel hydropower harvesting device. *In International Conference on MEMS, NANO and Smart Systems, ICMENS*, Aug 25-27, pp 480-485, Banff, Alta., Canada, 2004.
- [17] Dickson R.M. "New concepts in Renewable energy", <http://newrenewables.net/>, pp 33-34, 2008.
- [18] Li S and Lipson H. Vertical-stalk flapping-leaf generator for wind energy harvesting. *In ASME Conference on Smart Materials, Adaptive Structures and Intelligent Systems, SMASIS2009*, CA, United States, Sep 21-23, vol. No. 2, pp 611-619, 2009.
- [19] Hobeck J and Inman D.J. Energy harvesting from turbulence-induced vibration in airflow: Artificial piezoelectric grass concept. *In ASME Conference on Smart Materials, Adaptive Structures and Intelligent Systems, SMASIS*, Sep 18-21, AZ, United States, 2011.
- [20] Bryant M, Mahtani R and Garcia E. Synergistic wake interactions in aeroelastic flutter vibration energy harvester arrays. *In ASME Conference on Smart Materials, Adaptive Structures and Intelligent Systems, SMASIS*, Sep 18-21, AZ, United States, 2011.
- [21] Milne-Thompson L.M. *Theoretical Hydrodynamics* Macmillan, New York, 1960.
- [22] Glauert H. *Elements of Aerofoil and Airscrew Theory*. 2nd Edition, Cambridge University Press, Cambridge, U.K., 1997.
- [23] Wind Resources in Victoria, 2010, Sustainability Victoria, viewed 26/12 2011. <<http://www.sustainability.vic.gov.au/www/html/2111-wind.asp%3E>.

Copyright Statement

The authors confirm that they, and/or their company or organization, hold copyright on all of the original material included in this paper. The authors also confirm that they have obtained permission, from the copyright holder of any third party material included in this paper, to publish it as part of their paper. The authors confirm that they give permission, or have obtained permission from the copyright holder of this paper, for the publication and distribution of this paper as part of the ICAS2012 proceedings or as individual off-prints from the proceedings.